

SURFACE ACOUSTICS WAVE SENSOR BY USING PIEZOELECTRIC DEVICES

Rakesh kumar Pati¹ , S.k.mohammed ali¹, Sakuntala Mohapatra¹, Millee Panigrahi¹

1. MEMS Design Center , Electronics and Telecommunication Dept., Trident
Academy Of Technology, Bhubaneswar, Odisha,India

I. ACKNOWLEDGEMENT

The satisfaction and euphoria that accompany that successful completion of any task would be incomplete without mentioning the people who made it possible so, with gratitude I (Rakesh Kumar Pati) acknowledge all those guidance and encouragement made to successfully complete the project.

First and foremost I offer my sincere gratitude and respect to my advisor and guide Asst. Prof. Millee Panigrahi Trident academy of technology, who gave me the opportunity to do this project, whose keen interest and constant inspiration and valuable guidance helped in completion of the project. She gave her support to tide over potential dead ends and pitfalls.

Last but not the least I acknowledge the help provided by the department of Electronics and Telecommunication, TAT, Bhubaneswar which has been constant source of inspiration and strength to me.

SURFACE ACOUSTIC WAVE SENSOR USING PIEZOELECTRIC MATERIALS

II. ABSTRACT

Since 1985 when the first robot PUMA 560 was employed to place a needle during a brain CT biopsy, surgical robots have become ubiquitous in clinical surgeries. It is due to as a mechanical device the surgical robot possesses numerous advantages over human surgeons, therefore, is suitable in remote surgeries, minimally invasive surgeries and unmanned surgeries. Despite its advantages and success in surgeries, the interactions between the robot and the surgeons remain deficient, especially for the pressure sensing which plays an important role & again the interaction between the robot and the patient is still very limited. It is because till now the vision is almost the only feeling that a robot can have. The rigid endoscope camera is a common one used to track the robot motion. But for minimally invasive surgery (like close heart surgery, gastrointestinal surgery) where feeling tissue is critical to complete the operation. So a realistic sense of feel like our skin is at the forefront of research. Such a sensor could serve as a key component in artificial skin or be equipped on the end of a surgical robotic arm in the future. Inspired by the work of XINYU DU on bacterial sensing and design, fabrication, analysis, and evaluation of an innovative prototype pressure sensor based on Aluminum Nitride (AlN) Surface Acoustic Wave (SAW) and Shear Horizontal (SH)-SAW. In this project a SAW SENSOR is designed & a comparison is done using the different piezoelectric materials (ZnO, CdS & AlN).

The software tools used are 1) **Comsol Multiphysics** software tool & 2) Origin8.

III. INTRODUCTION:

During a robotic surgery, the robot holds and moves tools instead of human surgeons. Formally speaking a surgical robot is that “a powered computer controller manipulator with artificial sensing that can be reprogrammed to move and position tools to carry out a range of surgical tasks”. As a mechanical device the surgical robot possesses numerous advantages over human surgeons including stability, accuracy, precision, reliability and small incision, therefore, is suitable in remote surgeries, minimally invasive surgeries and unmanned surgeries.

Despite of the existing successful clinical applications, however, the interaction, i.e. artificial sensing, between the robot and the patient is still very limited. With the help of various cameras, vision is almost the only feeling that a robot can have. The rigid endoscope camera is a common one used to track the robot motion, monitor the operation process and provide a three dimensional view for surgeons. Although the vision feedback can do some help in complex tasks e.g. tying a suture, lacking of other feedbacks prevents the emergence of autonomous robots evolved from passive robots. For instance tactile and tensile feedbacks are desired by surgeons in a gastrointestinal surgery. Nevertheless by now surgeons can only rely on the video feedback from robots to estimate the tension exerted on the tissue. Another example is the minimally invasive surgery where feeling tissue is critical to complete the operation. In references a robot called “Da Vinci” system is developed by Intuitive Surgical Incorporated and employed in minimally invasive ‘closed’ heart surgery whose arm only carries an endoscope while other two arms carry scissors and grippers.

How to let a surgical robot possess **realistic sense of feel like** our skin is at the forefront of research. In order to imitate the human skin, various signals e.g. the strength of pressure, change of strength, speed and acceleration should be measured. All these signals are then processed with the help of artificial intelligent approaches to restore the tissue’s texture. Accurately measuring these physical signals is the basis of constructing an artificial skin so that a high precision pressure is desirable. In this work we will explore some design and fabrication techniques on an **effective sensor** which will be installed on our surgical robotic arm in the future.

CONTENTS

SL No.	Name	page no.
1	Acknowledgement	I
2	Abstract	II
3	INTRODUCTION	
4	Chapter 1 SURFACE ACOUSTICS WAVE SENSOR	
4.1	Introduction	
4.2	Pressure Sensor & SAW Sensor	
4.3	SAW Device Development	
4.4	Design	
4.5	Structure of SAW Device	
4.6	Detailed Geometrical Dimension & Other relevant selection	
4.7	Delta Function Analysis	
5	Chapter 2 Design of SURFACE ACOUSTICS WAVE SENSOR Using ComsolMultiphysics	
5.1	Introduction	
5.2	Model wizard	
5.3	Geometry	
5.4	Materials	
5.5	Study	
5.6	Results	
5.7	Point Evaluation	
5.8	Global Evaluation	
5.9	Conclusion	
5.10	References	

LIST OF ABBREVIATIONS

1. SAW-Surface Acoustics Wave
2. Al₂O₃- Aluminium Oxide

CHAPTER 1

SURFACE ACOUSTICS WAVE SENSOR

USING PIEZOELECTRIC DEVICES

INTRODUCTION:

Pressure Sensor & SAW sensor:

A pressure sensor is a transducer to convert the imposed pressure quantity to the electrical signal. Currently there exist various types of pressure sensors e.g. piezoresistive sensors, AIN BASED PRESSURE SENSORS, electromagnetic sensors, surface acoustic wave (SAW) sensors , optical pressure sensors, etc. Among all these types SAW sensors have unique superiorities which include but not limited to competitively **low cost, high sensitivity, intrinsically reliability, compact size and fast response in high dynamical environment**. Since the surgical robotic arm may bring the sensor into the human body where the sensor have to have the capability to operate in the liquid environment. The SAW mode existing in these sensors is normal to the sensor surface resulting in large attenuation in liquid environment. This intrinsic drawback can be overcome by using SH-SAW dual mode sensor. In the dual mode sensor, a strong shear-horizontal mode is found to coexist with the SAW mode which has the displacement parallel to the sensor surface so that the most energy is reserved even in the liquid environment. This property makes the dual mode device work in an aqueous environment without losing the high sensitivity as the SAW mode device. Recently, a type of dual mode devices based on the piezoelectric material Aluminum Nitride (AlN), have been designed, fabricated and successfully applied it in the application of bacterial sensing . As a natural extension, in this work, we will modify and apply **AlN-based, Zinc oxide based or Cadmium Sulphide sensor** in the surgical robotic application.

SAW DEVICE DEVELOPMENT:

SAW devices are some tools that utilize surface acoustic wave to generate electrical signal in response to some input quantities e.g. chemical concentrations, mass, relative humidity, pressure, temperature etc. For SAW devices SAW plays an important role that can couple with any media in contact with the surface of the device. This coupling strongly affects the amplitude and velocity of the SAW so that it allows the SAW device to detect the change of input quantities.

The most common way to generate or acquire SAW is utilizing the piezoelectric material where the mechanical and electrical fields are coupled at the atomic level. There are two SAW-related phenomena intrinsic in piezoelectric materials: direct piezoelectric effect and converse piezoelectric effect. The direct piezoelectric effect is that the material can generate electric potential in response to mechanical stress applied. The converse piezoelectric effect means that a material produces the stress and strain when an electric field is applied.

SAW can be excited and detected efficiently by using comb-like electrodes named IDT placed on the surface of a piezoelectric substrate. Thence forward, a vast amount of effort was put into the research and development of SAW devices and the SAW devices were widely used in electronic circuits as filters, oscillators and transformers, e.g. by now all TV receivers have SAW filters.

In the late 1970s, Wohltjen and Dessy [30] designed and applied the SAW delay line device for chemical vapor sensing. For such a sensor SAW is generated and acquired by IDT at each end of the device. The chemical object then can be detected according to the change of the output electrical signal in terms of frequency or phase. More recently, the SAW sensors have been improved significantly and extensively applied to diverse fields due to its small size, low cost, high sensitivity and wide variety of measurement.

There exist variety of piezoelectric materials, natural or manmade each of which possess distinct properties and advantages. A comparison between various materials on piezoelectricity is listed in the Table 3.1. Quartz (crystalline SiO₂) is one of common natural piezoelectric materials. The main advantage of quartz is the low temperature coefficient compared to other common piezoelectric materials. The price is relatively low due to its widespread usage.

Zinc Oxide (ZnO) and Aluminum Nitride (AlN) are two particular materials for SAW sensors with thin film structure. ZnO has relatively high electromechanical coupling coefficient and widely used in the field of ultrasonic transducers.

Substrate (Substrate Cut)	v (m/s)	K_{v2} (%)
Quartz (ST, X)	3158	0.11
Lithium Niobate (-Y, Z)	3488	4.8
Gallium Arsenide (Z, X+22.5)	2763	0.022

Table 3.1 The comparison between various piezoelectric material on wave velocity, mechanical properties and piezoelectric coefficients.

Density	5684[kg/m ³]	kg/m ³
Elasticity matrix (Ordering: xx, yy, zz, yz, xz, xy)	{9.06835e+010[Pa], 5.8089e+010[Pa], 9.06835e+010[Pa], 5.09351e+010[Pa], 5.09351e+010[Pa], 9.38047e+010[Pa], 0[Pa], 0[Pa], 0[Pa], 1.50399e+010[Pa], 0[Pa], 0[Pa], 0[Pa], 0[Pa], 1.50399e+010[Pa], 0[Pa], 0[Pa],	Pa

	0[Pa], 0[Pa], 0[Pa], 1.62973e+010[Pa]}	
Coupling matrix	{0[C/m ²], 0[C/m ²], -0.219231[C/m ²], 0[C/m ²], 0[C/m ²], -0.219231[C/m ²], 0[C/m ²], 0[C/m ²], 0.456838[C/m ²], 0[C/m ²], -0.210558[C/m ²], 0[C/m ²], - 0.210558[C/m ²], 0[C/m ²], 0[C/m ²], 0[C/m ²], 0[C/m ²], 0[C/m ²]}	C/m ²
Relative permittivity	{9.0171, 9.0171, 9.5210}	1

Table 3.2 various properties of Cadmium Sulphide

Name	Value	Unit
Density	3300[kg/m ³]	kg/m ³
Elasticity matrix (Ordering: xx, yy, zz, yz, xz, xy)	{4.1e+011[Pa], 1.49e+011[Pa], 4.1e+011[Pa], 9.9e+010[Pa], 1.49e+011[Pa], 3.89e+011[Pa], 0[Pa], 0[Pa], 0[Pa], 1.25e+011[Pa], 0[Pa], 0[Pa], 0[Pa], 0[Pa], 1.25e+011[Pa], 0[Pa], 0[Pa], 0[Pa], 0[Pa], 0[Pa], 1.25e+011[Pa]}	Pa
Coupling matrix	{0[C/m ²], 0[C/m ²], -0.58[C/m ²], 0[C/m ²], 0[C/m ²], -0.58[C/m ²], 0[C/m ²], 0[C/m ²], 1.55[C/m ²], 0[C/m ²], -0.48[C/m ²], 0[C/m ²], -0.48[C/m ²], 0[C/m ²], 0[C/m ²], 0[C/m ²], 0[C/m ²], 0[C/m ²]}	C/m ²
Relative permittivity	9	1

Table 3.3 Various parameters of Aluminium Nitride

Name	Value	Unit
Density	5680[kg/m ³]	kg/m ³
Elasticity matrix (Ordering: xx, yy, zz, yz, xz, xy)	{2.09714e+011[Pa], 1.2114e+011[Pa], 2.09714e+011[Pa], 1.05359e+011[Pa], 1.05359e+011[Pa], 2.11194e+011[Pa], 0[Pa], 0[Pa], 0[Pa], 4.23729e+010[Pa], 0[Pa], 0[Pa], 0[Pa], 0[Pa], 4.23729e+010[Pa], 0[Pa], 0[Pa], 0[Pa], 0[Pa], 0[Pa], 4.42478e+010[Pa]}	Pa
Coupling matrix	{0[C/m ²], 0[C/m ²], -0.567005[C/m ²], 0[C/m ²], 0[C/m ²], -0.567005[C/m ²], 0[C/m ²], 0[C/m ²], 1.32044[C/m ²], 0[C/m ²], -0.480508[C/m ²], 0[C/m ²], - 0.480508[C/m ²], 0[C/m ²], 0[C/m ²], 0[C/m ²], 0[C/m ²], 0[C/m ²]}	C/m ²
Relative permittivity	{8.5446, 8.5446, 10.204}	1

Table 3.4 Various parameters of Aluminium Nitride

THE DESIGN AND THEORETICAL ANALYSIS OF THESA W DEVICE

The proposed pressure sensor consists of three parts: rubber probe, AlN based SAW device and circuit board which are shown in Fig. 3.1. Here the cylinder-like rubber probe is attached to the plastic support which is fixed on the circuit board. It can prevent the hard surface of the device from scratching the body tissue. The gap between the probe and the device surface provides the pressure sensor an adjustable offset which will omit the tiny disturbance and increase the stability of the measurement. The constant contacting area makes the pressure reading only depend on the exerted force therefore more consistent.

The **AlN-based SAW device** can convert the change of pressure exerted on the surface into the change of electrical signal's signature (e.g.frequency, phase, amplitude, etc.). When the device is in contact to the patient's body tissues, the electrical signal out of the device will be changed accordingly. By controlling the motion of robotic arm, the information combining force and speed can be collected and analyzed by the signal processing and machine learning model in the robot or remote controller. The textile or hardness can be thereby extracted. The electrical circuit board is the base of the device as well as provides the functions for excitation signals, conditioning signals and transmitting signals.

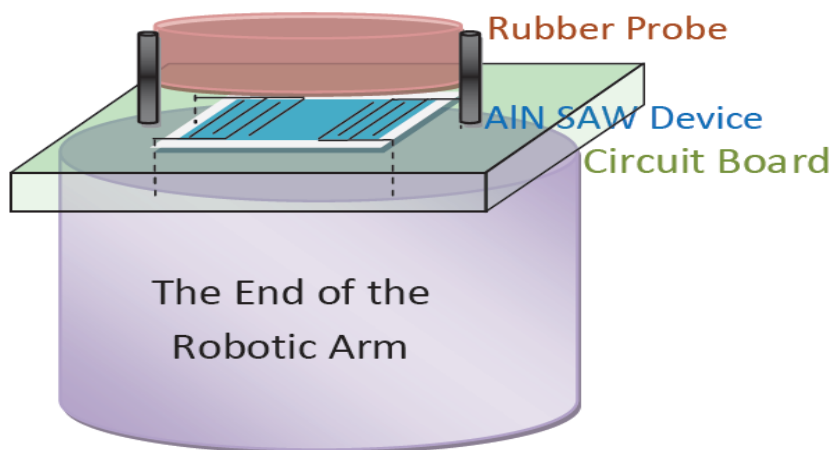
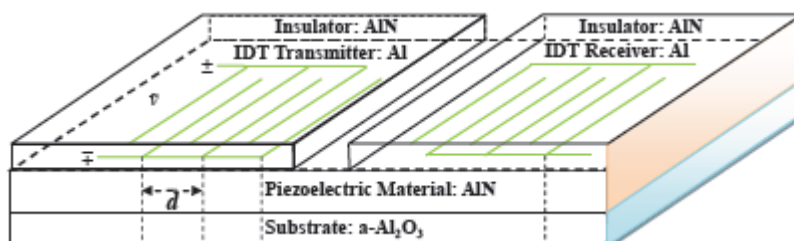


Fig 3.1The schematics of a prototype AlN-based SAW sensor

2.1 The Structure of the SAW Device

The structure of the proposed AlN-Based SAW device is shown in the Fig. 3.2.This sandwich-like device includes substrate, piezoelectric material, metal IDT.



Excerpt from the Proceedings of the 2013 COMSOL Conference in Bangalore

Fig 3.2 Structure of a SAW Device

In crystallography, the Miller indices is extensively used to specify planes and directions which includes three integers l , m and n written as $(l\ m\ n)$. By convention, negative integers are written with a bar, e.g. $\bar{1}$ for -1. All three integers are usually written in the lowest term, i.e. their greatest common divisor should be 1. A plane $(l\ m\ n)$ means that it intercepts three axes at l , m , n , or some multiple thereof, respectively. The value 0 means the plane do not intersect that axis. For hexagonal structures, a four index scheme called Bravais-Miller index $(h\ k\ i\ l)$ is used to label planes. Here h , k and l are identical to the Miller index, is a redundant index which is equal to $-h-k$. For example, the A plane in Fig. 2.3 intercepts x and y axis at 1 and parallel with z axis.

Hence, $h = k = 1$, $i = -h-k = -2$ and $l = 0$.

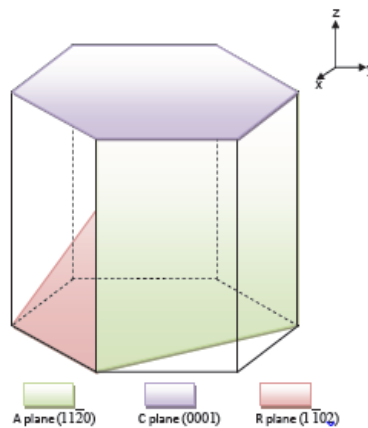


Fig 3.3 The typical plane orientation
in the unit cell of sapphire

1. Aluminum Oxide

Several substrates can be used for AlN growth, e.g. Si, SiC, GaN, ZnO, MgO etc. SiC is considered as the best substrate for AlN heteroepitaxy growth since the lattice mismatch with AlN is only 3.5%. Its drawback is the extreme high price (\$USD1090 for one 3-inch wafer in 2008). Today sapphire (Aluminium Oxide) is the most popular substrates for synthesizing heteroepitaxial AlN growth due to the adequate thermal and chemical stability at high growth temperatures, excellent structural and surface morphology and availability in large quantities. Three major orientations of Aluminium nitride have been used which are C plane (0001), A plane (1120) and R plane (1 102) shown in Fig. 3.3. The crystal orientations of sapphire and AlN are parallel but the lattice mismatch with AlN is about 12%. Note that sapphire is also an anisotropic material, therefore, different cut of substrate make the device different. It was found in that the AlN-based device growing on A

plane sapphire has the capability to work in aqueous environment due to the existence of SH-SAW mode. Overall our AlN based SAW device will be grown on A plane sapphire.

2.IDT

There are two ends for IDT, transmitter end and receiver end. Generally, they are geometrically symmetric. When a radio-frequency (RF) voltage $v\sim$ is connected to the IDT transmitter end, each pair of transducer finger may be considered to be a discrete power source. All fingers on the top side or bottom side have the same electrical potential since they are connected with the same electrode. The piezoelectric substrate underneath the fingers with the same electrical potential will have the same strain. Therefore, an acoustic wave will be generated in the substrate (e.g. acoustic wave 1 shown in Fig. 2.4). The wavelength λ of the acoustic wave is equal to the distance between two adjacent IDT pairs d since the wavelength is defined as the distance between consecutive corresponding points of the same phase, that is

$$\lambda = d \quad \text{.....3.1}$$

The frequency f_0 of the acoustic wave is [52],

$$f_0 = \frac{1}{T} = \frac{v}{\lambda} \quad \text{.....3.2}$$

Take (2.2) into (2.1), we have

$$f_0 = \frac{v}{d} \quad \text{.....3.3}$$

Where v is phase velocity of the acoustic wave about 5740 m/s for AlN which is determined by substrate materials (some materials are listed in Table 3.1). Since AlN is an anisotropic material, the velocity can be varied along different propagation direction. It is also worth noting that the electromagnetic wave is five orders of magnitude faster than the acoustic wave, the dimension of the device only relying on electromagnetic wave has to be five orders smaller than the acoustic wave device.

Since the metal IDT is conductive, it is necessary to coat an insulator layer over the IDT to make the device working in aqueous environment. It was concluded that the insulator layer brings additional attenuation resulting in performance deterioration. In our work, two improvements are made. First the insulator layer does not cover the whole area of the top surface, instead only the IDT and electrodes areas are covered. Second, inspired by the design in where the IDT are placed between the substrate and piezoelectric material in a ZnO-based SAW device another layer of AlN is coated though such a design brings some technical difficulties due to different melt temperature in AlN and Al IDT.

The Detailed Geometrical Dimensions and Other Relevant Selection:-

After determining the structure and material of the device, the detailed geometry should be defined before fabrication. Some considerations which will be stated below the dimensions of IDT are chosen as shown in Table 3.5. According to Equations 3.1- 3.4 and other considerations which will be stated below the dimensions of IDT are chosen as shown in Table 3.5. An intuitive description of the whole device is shown in Fig. 3.2. Note that for better virtualization the size of the plot in Fig. 3.2 is not directly proportional to the real size.

IDT finger width	6 μm
IDT finger length	1680 μm
Distance between two adjacent IDT fingers	6 μm
Distance between transmitter and receiver IDT	3606 μm
Electrode width	720 μm
Distance between electrodes	1760 μm
Insulator width	3400 μm
Insulator length	4240 μm

Table 3.5 Relevant Parameters & there length

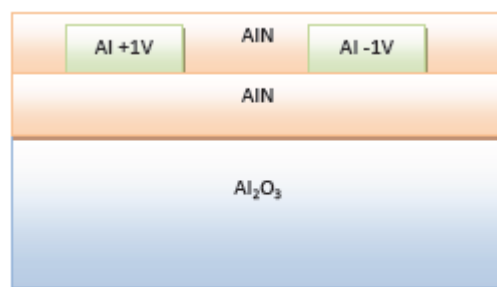


Fig 3.4 The device schematic plots: (a) on x-z plane

In order to enhance the device performance, one modification is made on the original design. Each IDT finger is split into two fingers to reduce the pass band ripples. The width of each modified finger becomes half of the original width. The pass band ripple is caused by multiple reflections within and between the IDT fingers.

2.3. Delta Function Model Analysis of the Device

The Delta function model is an impulse response analysis. It has been widely applied on different types of SAW devices to achieve qualitative results [55]. Generally a linear time invariant (LTI) system is able to be characterized completely by its impulse response $h(t)$ since the response to other arbitrary signal for a LTI system can be represented by $h(t)$. Therefore, we derive the impulse response $h(t)$ for a SAW device here, and then obtain its frequency response $H(f)$. In this way, we can investigate the frequency characteristics for a SAW device.

Suppose that an impulse input (+V, -V) is connected to the IDT transmitter end each IDT finger will generate an impulse signal with the amplitude A and -A (shown in Fig. 2.5). The amplitude A is a constant and determined by piezoelectric material and substrate's properties. Note that the impulse inputs can not be (+V, 0) since it's contradictive to our assumption that the polarity of two adjacent IDT fingers is opposite. As a result, the output of the IDT transmitter is a series of impulse signal (i.e. SAW) with the period T/2 and amplitude A and -A. Here the attenuation of amplitude A caused by the substrate is omitted.

Since the impulse response function $h(t)$ is discrete in time, we use $h(n)$ to represent $h(t)$ and the corresponding discrete-time frequency response $H(f)$ can be calculated according to the inverse discrete-time Fourier transform equation,

$$H_T(f) = \sum_{n=-\infty}^{\infty} h(n)e^{-j\pi n f T}$$

$$H_T(f) = -A \sum_{n=0,2}^{2N-2} e^{-j\pi f T n} + A \sum_{n=1,3}^{2N-1} e^{-j\pi f T n}$$

It has been found

1. If we increase the number of IDT finger pairs the bandwidth will become narrower.
2. The phase delay depends on N, T, L and v. If we increase N, T or L or decrease v the phase delay will be increased.

2.4. Structural Mechanics Analysis of the Device

As we discussed above, the SAW sensor is a class of acoustic wave devices. The input electrical signal excites the acoustic wave by piezoelectric materials, and passes through the device. The acoustic wave is sensitive to the force exhibited on the device and converted to the electrical signal by

piezoelectric material. Therefore, to derive the mathematical model of the whole device, the surface acoustic wave propagation should be derived at first.

As an elastic material, either for Al₂O₃ or AlN, the wave equations are determined by the internal stress and strain. The stress inside the body is caused by an applied load on the body exterior. One can imagine that two adjacent blocks inside the body exert the internal force on each other across an imaginary plane of separation. When the force is parallel to this plane it is called shear stress. When the force is normal to it, it is normal stress. The stresses derive from the cohesive nature of the body's material. With the normal stress, the size of an element in a body will be changed which is called simply strain. With the shear stress, the edge angle of an element in a body will be changed which is known as shear strain. According to the Hooke's law, the materials which are considered as elastic are governed by the two following equations,

$$\sigma = E\varepsilon$$

$$\tau = G\gamma$$

Where E is Young's modulus and G is modulus of rigidity. They are the intrinsic elastic properties for a material. These two equations completely characterize the elastic behavior of a solid in the small deformation limit (strain is less than 10⁻⁵). In the three-dimensional space the normal stress (strain) and shear stress (strain) for any one point in the body will have multiple components as shown in Fig. 3.2. For better presentation, Cauchy stress tensor T is used to define all stress components and strain tensor S for all strain components which were introduced by Cauchy around 1822, that is,

$$T = \begin{bmatrix} T_{xx} & T_{xy} & T_{xz} \\ T_{yx} & T_{yy} & T_{yz} \\ T_{zx} & T_{zy} & T_{zz} \end{bmatrix}, S = \begin{bmatrix} S_{xx} & S_{xy} & S_{xz} \\ S_{yx} & S_{yy} & S_{yz} \\ S_{zx} & S_{zy} & S_{zz} \end{bmatrix} \quad \text{.....3.5}$$

Each component of T is denoted by two subscripts, the first denoting the direction of the force and the second denoting the direction of the area. The component of strain S also has two subscripts. If the two subscripts are the same, the stress and strain are the normal stress and strain i.e. the change is perpendicular to the surface. Otherwise, it is a shear stress (or strain) in two different direction indicated by the two subscripts i.e. the change is parallel to the surface.

Equations Involved in Mathematical Model Analysis

For the piezoelectric material AlN, the mathematical model should contain two more field variables, electric flux density D and electric field intensity E . According to the electromagnetic theory, the quantities D and E are related by material electrical permittivity, that is

$$D = \epsilon E \quad \dots\dots\dots 3.6$$

However, for piezoelectric material where the structure of crystal lacks a center of inversion symmetry, the strain changes result in the change of the charge distribution that produces the electrical polarization. This is called direct piezoelectric effect and can be described by,

$$D = eS + \epsilon E \quad \dots\dots\dots 3.7$$

Where e =Piezoelectric stress constant Matrix having unit charge/(length)²

If we consider quasi-electrostatic approximation then

$$\nabla \times E = 0$$

The electric field E can be expressed as the function of electric potential, that is

$$E = -\nabla \phi$$

where ρ is the charge density and is usually negligible in piezoelectric materials.

CHAPTER 2

SAW WAVE SENSOR DESIGN

USING COMSOL

INTRODUCTION:

In this chapter main emphasis is made on the main design of AIN Based pressure sensor using Comsol Multiphysics. All the design steps are discussed as follows.

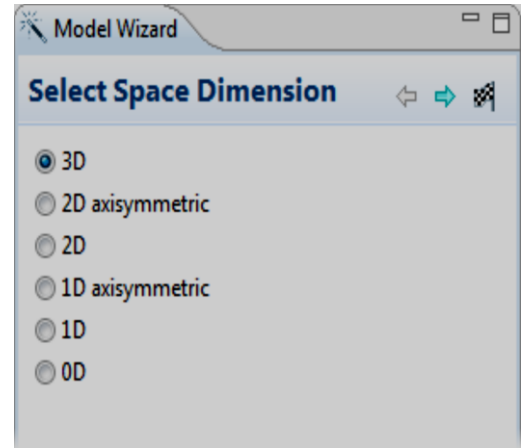
MODEL WIZARD

1. Open the **Model Wizard**. To open the Model Wizard, double-click the COMSOL icon on the desktop Or when COMSOL is already open,

- Click the **New button** on the main toolbar

-Select File>New from the main menu

-Right-click the root node and select **Add Model** Fig 4.1 Model Wizard



2. When the Model Wizard opens, select a

Space dimension; the default is 3D. Click the

Next button.

3. In the **Add Physics** window, click the **ac/dc** folder, then right-click **electrostatics** and choose **Add Selected**. Click the **Next** button .

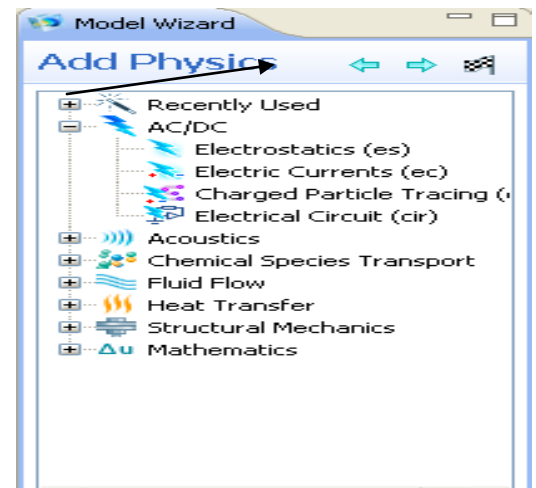


Fig 4.2 Add Physics Window

4. In the Select **Study** Type window, click to select the **Stationary** study type. Click the **Finish** button.

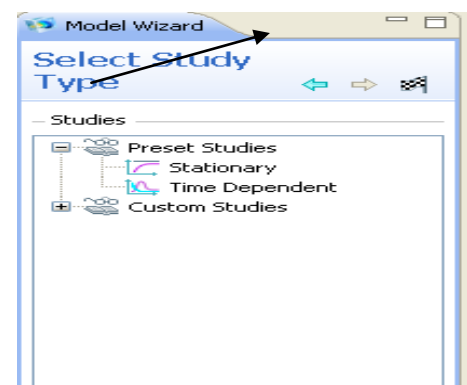


Fig 4.3 Study type Window

GEOMETRY:

In this design we are designing all the geometry by our own rather than importing from a predefined library. It is done as per following process.

1. In the Model Builder window click on model1->Definitions->Geometry.
2. Right click on geometry 1 and chose Block
3. Give the dimensions of the 1st block (In the Size field :-- Width=5, Height=1. In the Position edit field:-- $x=0m$, $y=0m$).
4. Now Click on Build Selected. Click on Zoom Extent. Fig 4.4 Selecting block
The figure appears as below:

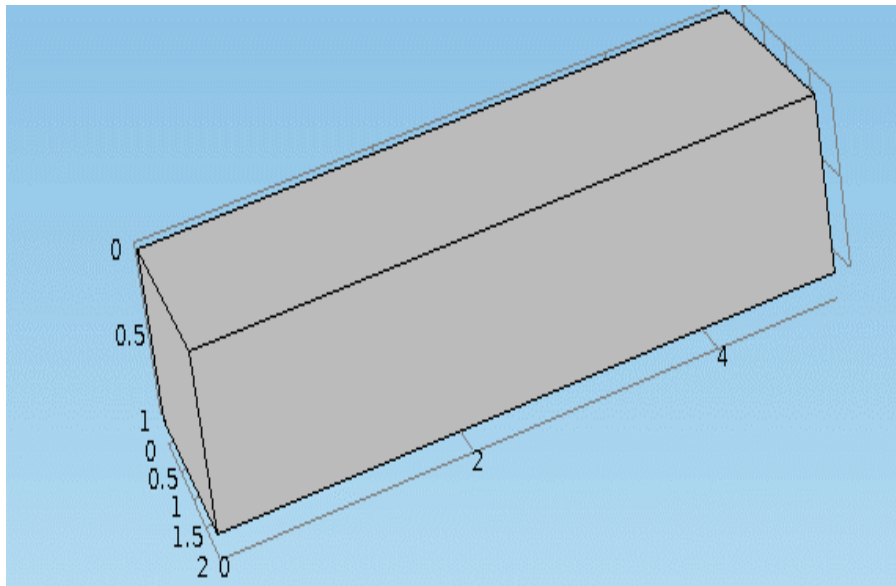
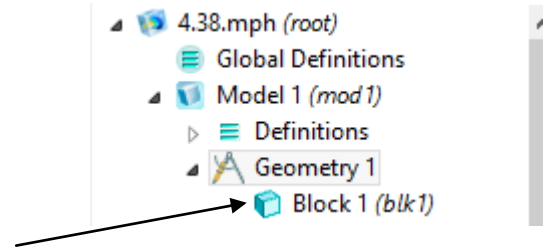


Fig 4.5 Block1

5. Similarly build other blocks of dimensions as given below:-

Block-2(Size:-- Width=5m, Height=0.5m depth=2m& Position:-- $x=0m$, $y=0m$, $z=1m$)

Block-3(Size:-- Width=1.3m, Height=1m, depth=2m& Position:-- $x=0m$, $y=0.0$ & $z=1m$)

Block-4(Size:--Width=0.2m,Height=1m, depth=1.8m& Position:-- $x=0.1m$, $y=0.1m$ & $z=1.5m$)

Block-5(Size:--Width=0.2m,Height=1m, depth=1.8m & Position:-- $x=1m$, $y=0.1m$ & $z=1.5m$)

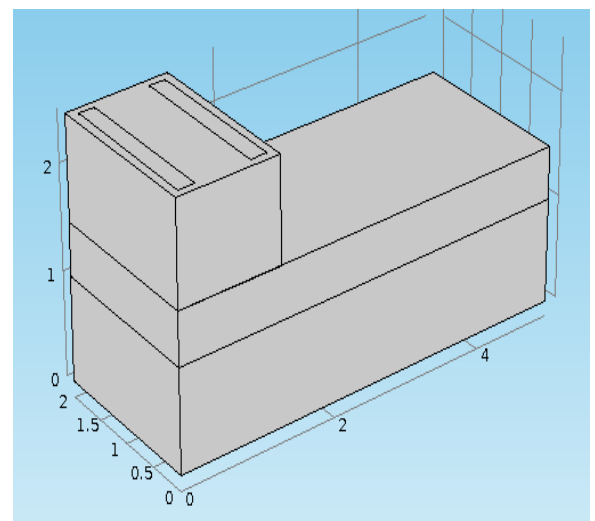


Fig 4.6 Block 1-6

To draw similar blocks we have to use array.

6. Right click on geometry, and then select transforms->array.
7. Go to Array Settings Window, Select Blockp-3,4& 5 as Input objects. In size edit field $x=2$, $y=3$. In Displacement edit field $x=3.7$ m.Click on Build select.

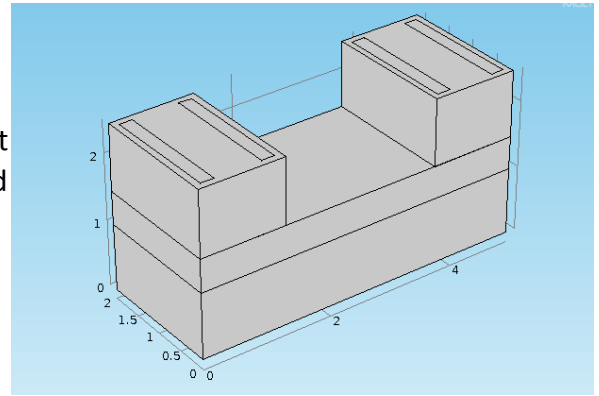


Fig 4.7 Replica of block 3,4,5 using array

8. Create another Block as Block6(Size:-- Width=5m, Height=0.2 m depth=2m & Position:-- $x=0$ m, $y=0$ m, $z=2$ m)

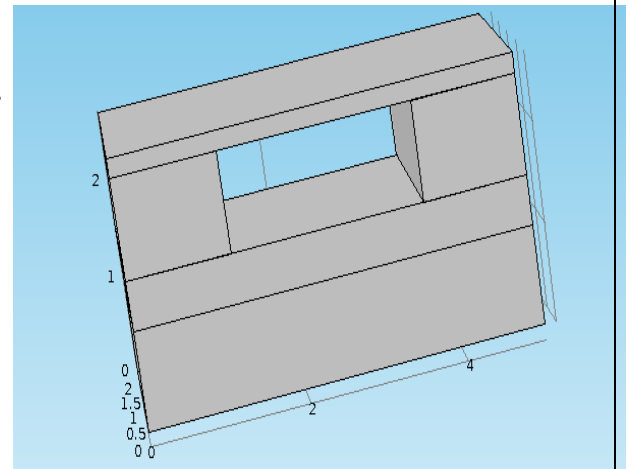


Fig 4.8 Complete block diagram

Now form the union to complete geometry.

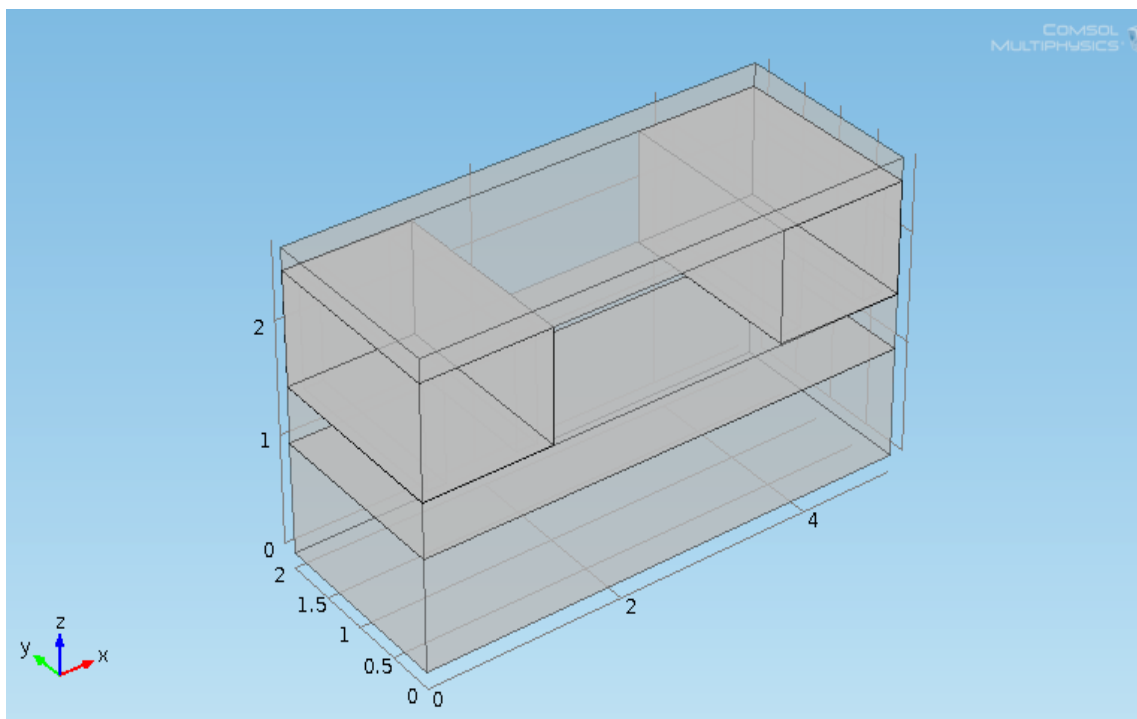
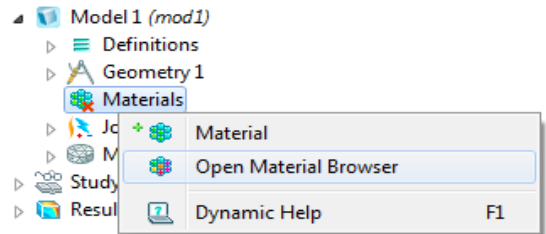


Fig 4.9 Complete Geometry

MATERIALS:

The Materials node stores the material properties for all physics and domains in a Model node. In this section different materials are added to the model as per its requirement as follows.

1. In the **Model Builder**, right-click **Materials** and select **Open Material Browser** (or select **View>Material Browser**).
2. Right click on MEMS>Insulator>Al2O3 and chose add material to the model.



3. Go to **Material settings** window. Select only domain 1 that is the substrate. In the Material content window check the values assigned.

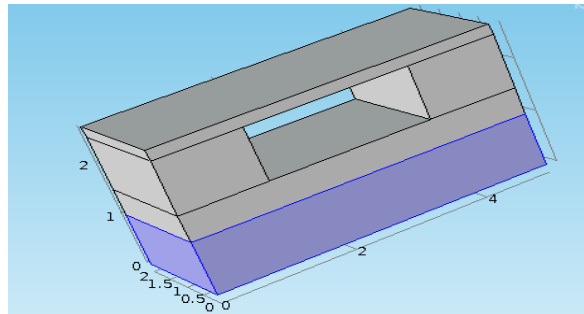


Fig 4.10 Al2O3 applied to domain 1

Name	Value	Unit
Density	3965[kg/m ³]	kg/m ³
Elasticity matrix (Ordering: xx, yy, zz, yz, xz, xy)	10	Pa
Coupling matrix	{2, 5, 5, 4, 5, 6, 9, 1, 8, 3, 5, 0, 4, 0, 4, 7, 8, 9}	C/m ²
Relative permittivity	1	1

Table 4.01 Material properties Al2O3

4. Again chose material browser. Right click on Pizeoelectric devices->Aluminium Nitride and chose **add material** to the model. Go to **Material settings** window. Select only domain 2,3,4& 7 that is the substrate. In the Material content window check the values assigned.

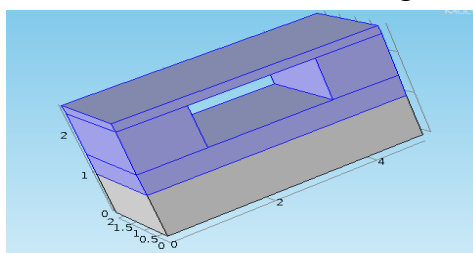


Fig 4.11 Aluminum Nitride applied to domain 2,3,4,7

Name	Value	Unit
Density	3300[kg/m ³]	kg/m ³
Elasticity matrix (Ordering: xx, yy, zz, yz, xz, xy)	{4.1e+011[Pa], 1.49e+011[Pa], 4.1e+011[Pa], 9.9e+010[Pa], 1.49e+011[Pa], 3.89e+011[Pa], 0[Pa], 0[Pa], 0[Pa], 1.25e+011[Pa], 0[Pa], 0[Pa], 0[Pa], 0[Pa], 1.25e+011[Pa], 0[Pa], 0[Pa], 0[Pa], 0[Pa], 0[Pa], 1.25e+011[Pa]}	Pa
Coupling matrix	{0[C/m ²], 0[C/m ²], -0.58[C/m ²], 0[C/m ²], 0[C/m ²], -0.58[C/m ²], 0[C/m ²], 0[C/m ²], 1.55[C/m ²], 0[C/m ²], -0.48[C/m ²], 0[C/m ²], - 0.48[C/m ²], 0[C/m ²], 0[C/m ²], - 0.48[C/m ²], 0[C/m ²], 0[C/m ²], 0[C/m ²], 0[C/m ²], 0[C/m ²]}	C/m ²
Relative permittivity	9	1

Table 4.2 material properties Aluminium Nitride

5. Again chose material browser. Right click on Built in->Aluminium and chose **add material** to the model.Go to **Material settings** window. Select only domain 5,6,8& 9 that is the substrateIn the Material content window check the values assigned.

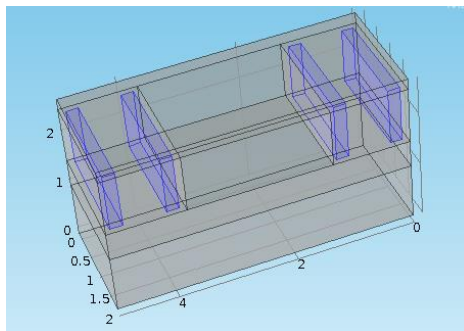


Fig 4.12 Aluminum applied to Domain 5,6,8,9

Name	Value	Unit
Density	2700[kg/m ³]	kg/m ³
Elasticity matrix (Ordering: xx, yy, zz, yz, xz, xy)	{10.3e10, 10.3e10, 10.3e10, 5.1e10, 5.1e10, 5.1e10}	Pa
Coupling matrix	{10, 20, 30, 40, 50, 60, 70, 80, 90, 100, 110, 120, 130, 140, 150, 160, 170, 180}	C/m ²
Relative permittivity	1.7	1

Table 4.3 Material properties of aluminum

6. Also we can add Zinc Oxide, Cadmium sulphide in place of Aluminum Nitride for different analysis.

MESH ANALYSIS:

Mesh analysis is done to check the correctness of the model. The simplest way to mesh is to create an unstructured tetrahedral mesh. It is done as follows:

1. Go to Model 1->geometry 1->Right click on **mesh 1** and select Free Tetrahedral.
2. Go to Size settings window ->Select Predefined (if extra modification in meshing is not required. Unless one can select custom & can assign Max element size, Min element size, Max element growth rate, Resolution of Curvature, Resolution of narrow regions etc.)->Choose Extra fine-> Select Build All.
3. Wait for some extent & the following figure arises.

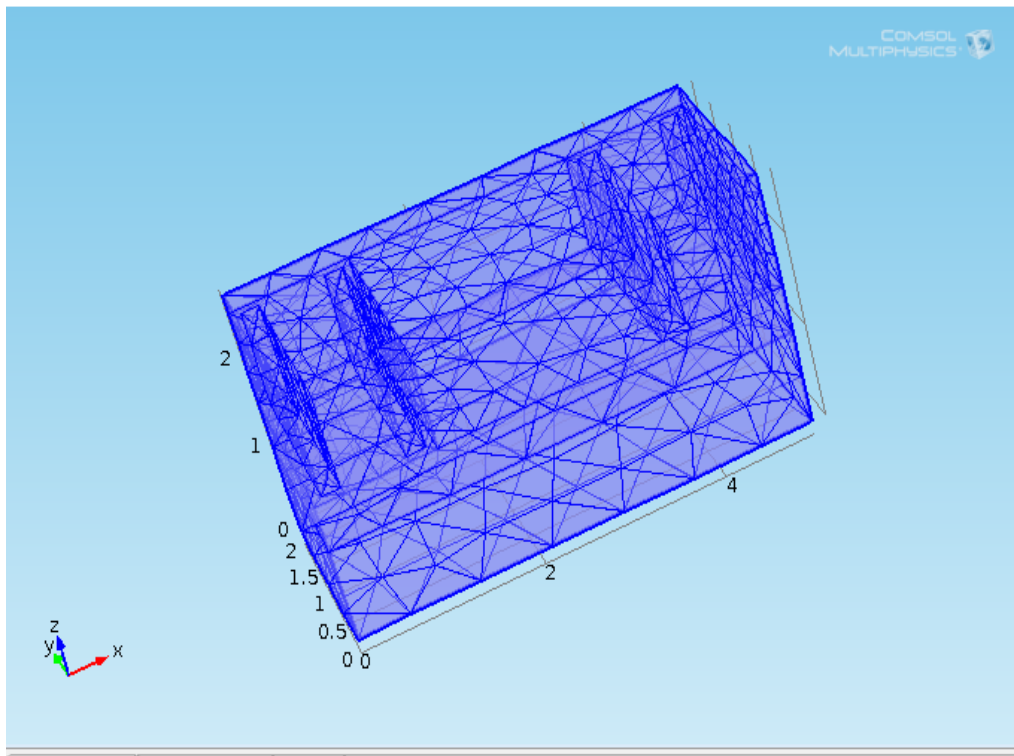


Fig 4.14 Mesh Analysis

STUDY:

The Study node automatically defines a solution sequence for the simulation based on the selected physics and the study type. The simulation only takes a few seconds to solve. The study of AlN based Pressure Sensor is made as per following process. Set Eigen frequency= $0.128e-6i$

1. In the **Model Builder**, right-click **Study 1** and choose **Compute**. Or press F8.
2. Wait for some extent the following analyzed figure arises.

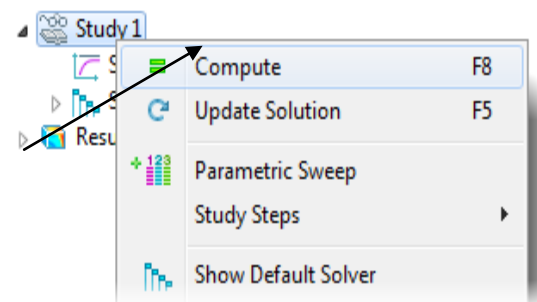


Fig 4.15 Study window

RESULTS:

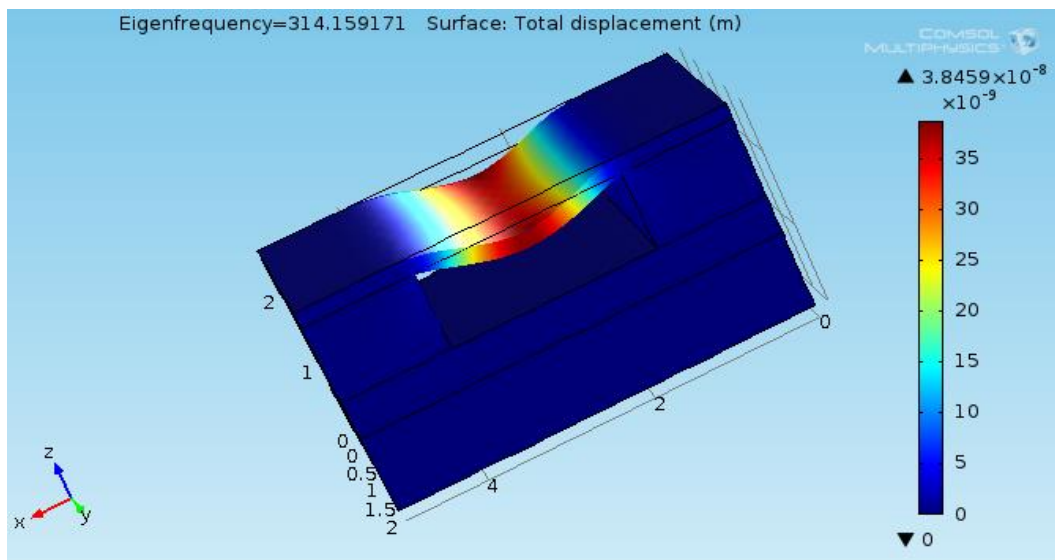


Fig 4.16 (using Aluminum Nitride)Eigen Freq. Vs Surface total displacement

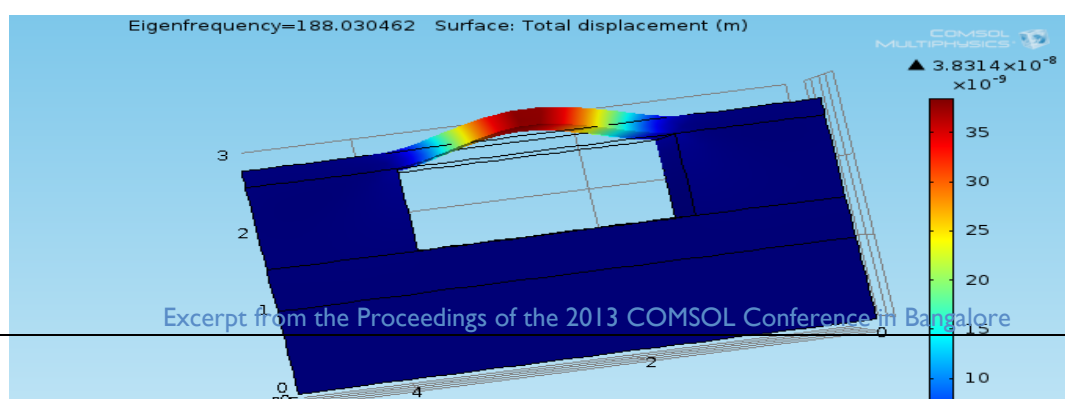


Fig 4.17(using Lithium Niobate) Eigen Freq. Vs Surface total displacement

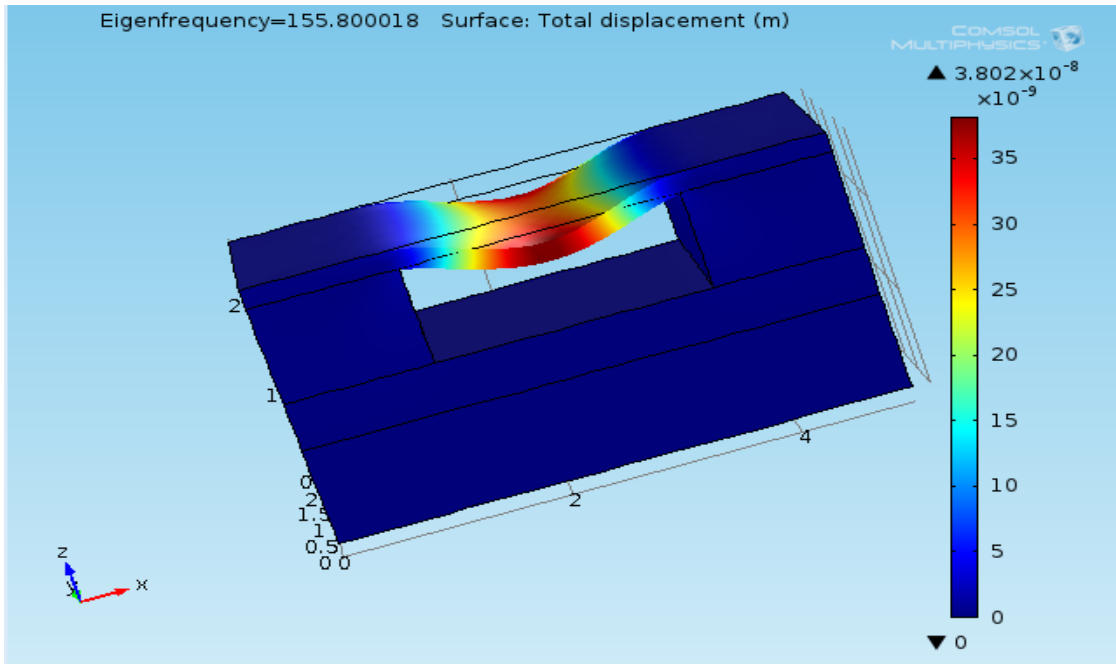


Fig 4.18(Using Zinc Oxide)Eigen Freq. Vs Surface total displacement

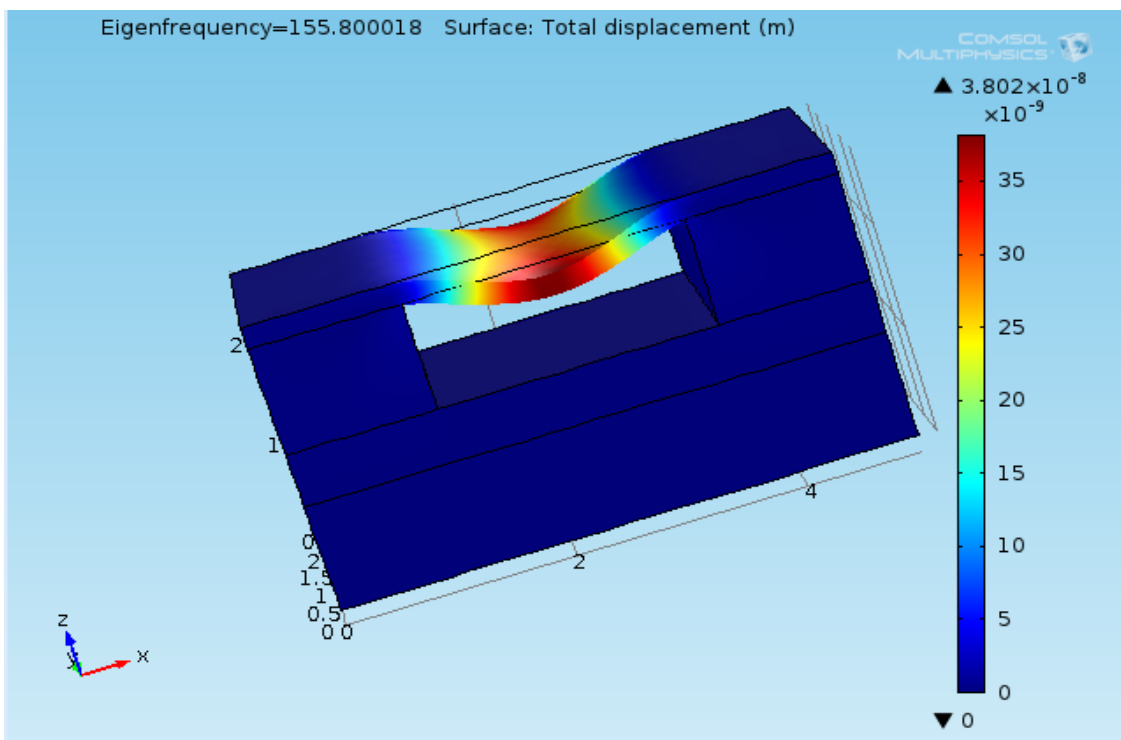


Fig 4.19(Using CadmiumSulphide)Eigen Freq. Vs Surface total displacement

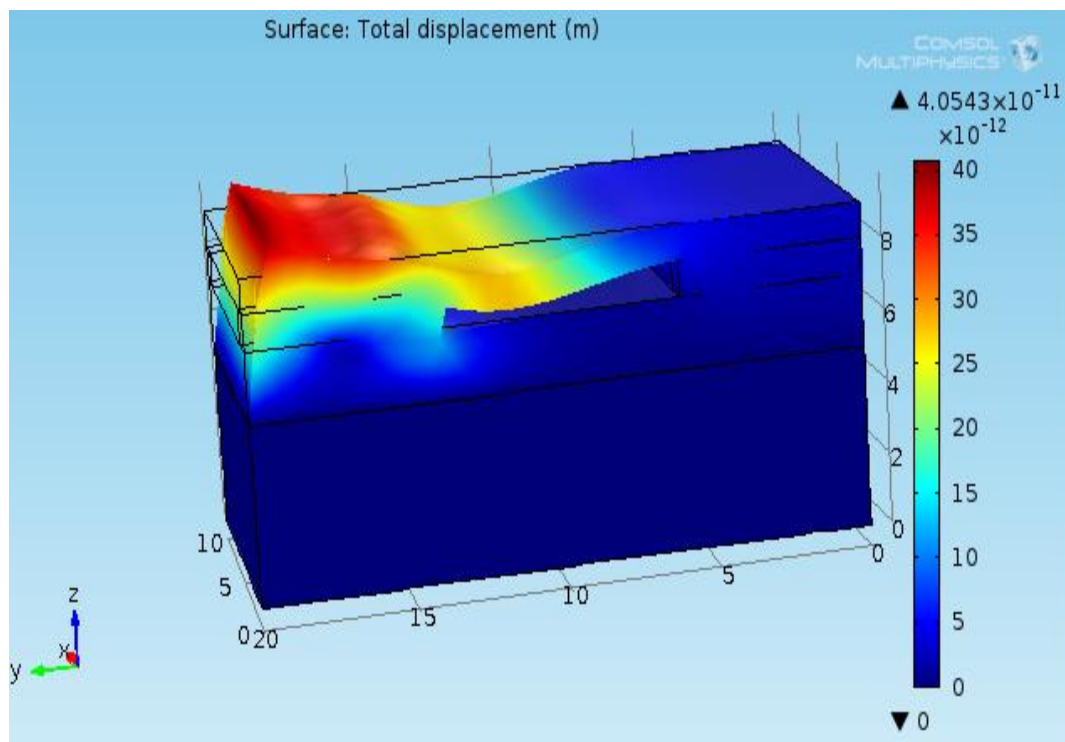


Fig. 4.20 Total Displacement in Time domain

POINT EVALUATIONS

1. Using Aluminum Nitride

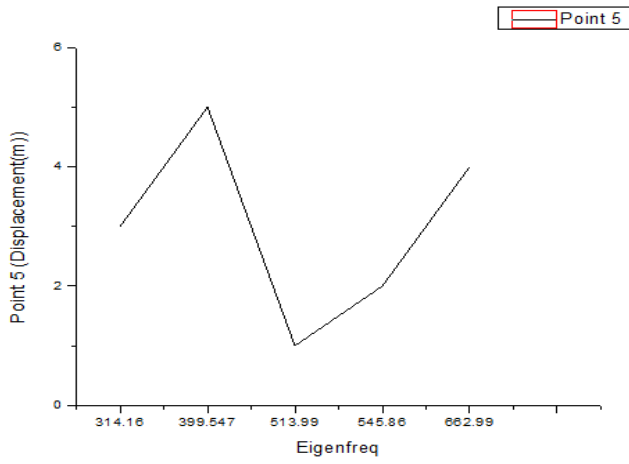


Fig 4.21 DispVs Eigen Freq.(point 5)

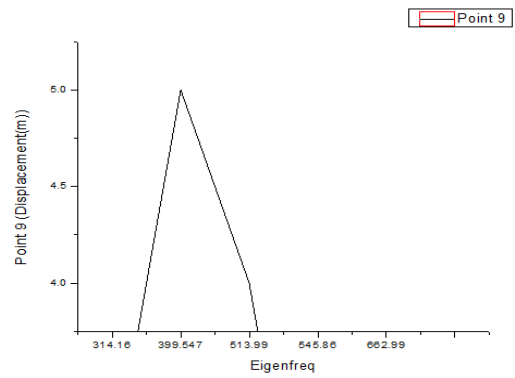


Fig 4.21 DispVs Eigen Freq.(point 9)

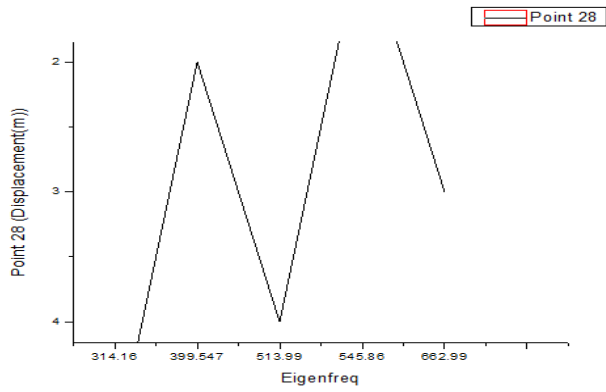


Fig 4.22DispVs Eigen Freq. (point 28)

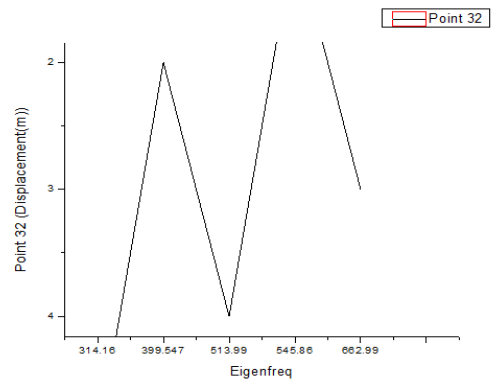


Fig 4.23DispVs Eigen Freq.(point 32)

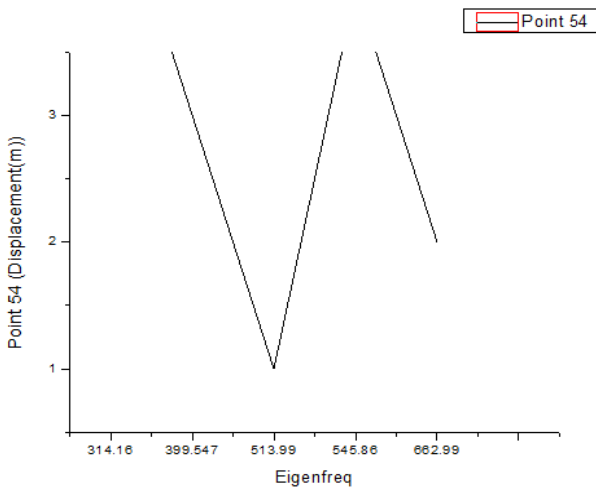


Fig 4.24DispVs Eigen Freq.(point 54)

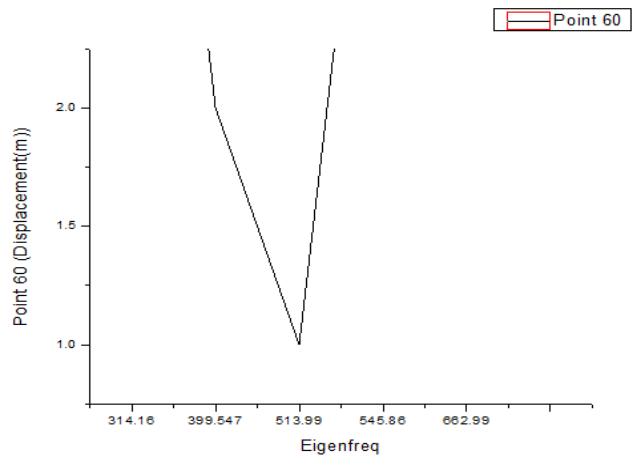


Fig 4.25DispVs Eigen Freq.(point 60)

2.Using Cadmium Sulphide

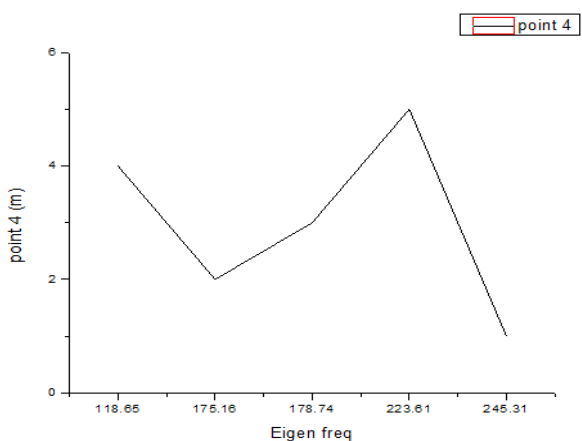


Fig 4.25 DispVs Eigen Freq.(point 4)

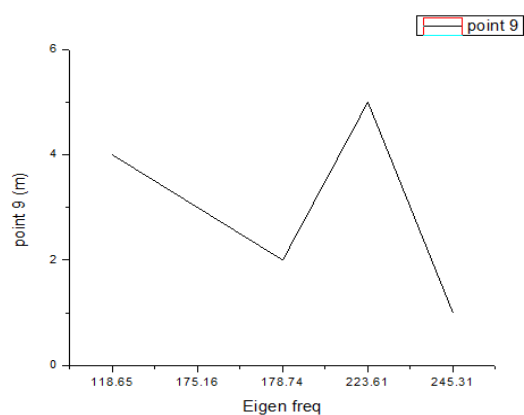


Fig 4.26 DispVs Eigen Freq.(point 9)

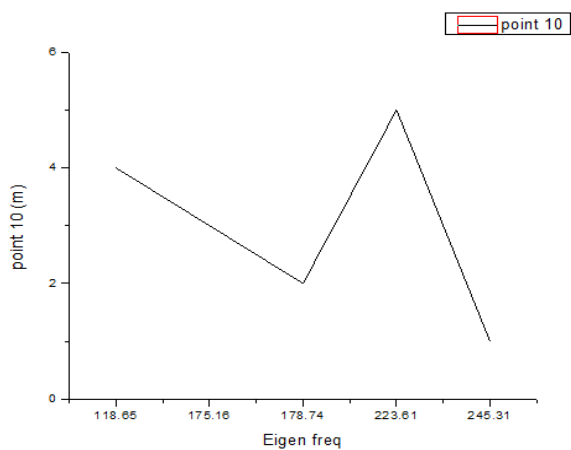


Fig 4.27 DispVs Eigen Freq.(point 10)

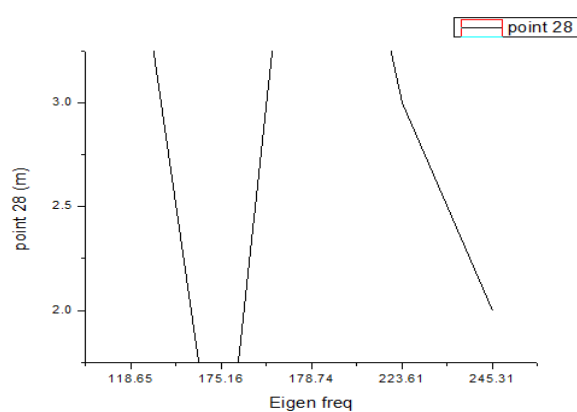


Fig 4.28 DispVs Eigen Freq.(point 28)

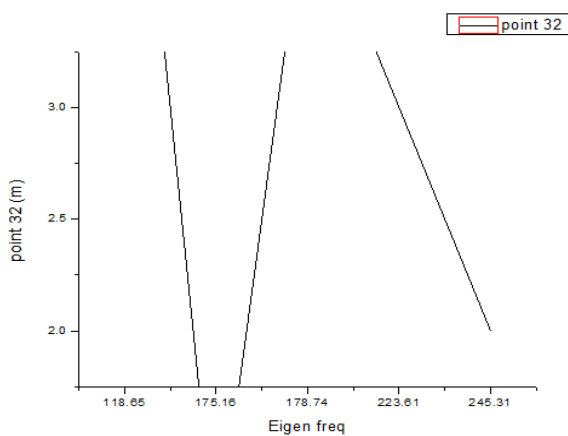


Fig 4.29 DispVs Eigen Freq.(point 32)

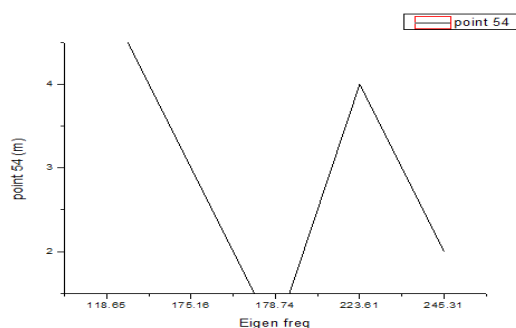


Fig 4.30 DispVs Eigen Freq.(point 59)

GLOBAL EVALUATIONS:

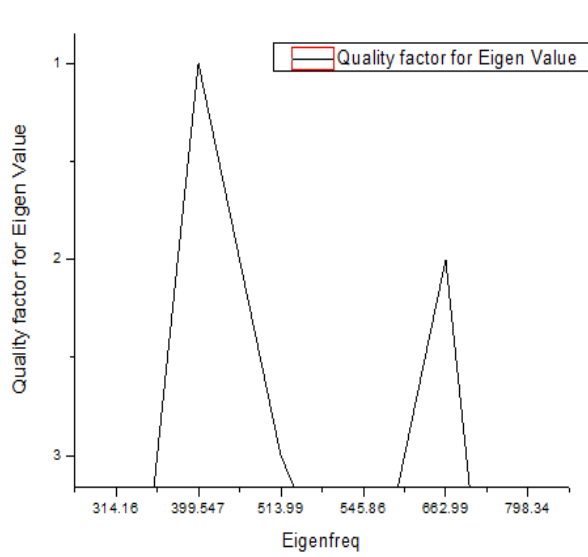


Fig 4.31 Quality Factor Vs Eigen Freq.

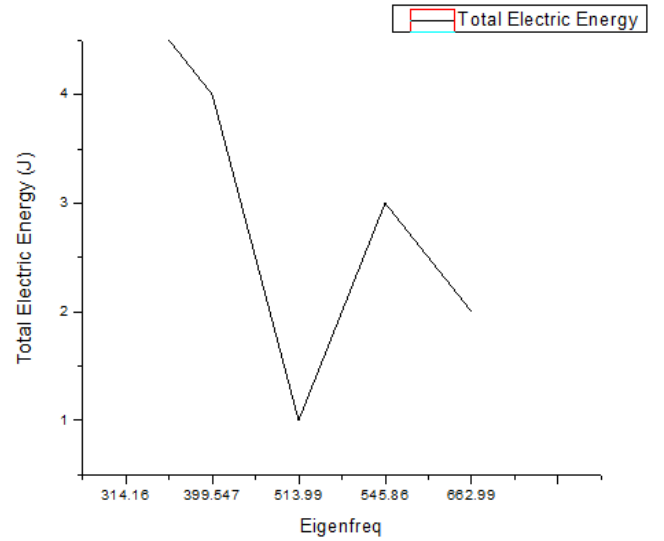


Fig 4.32 Total K.E. Vs Eigen Freq.

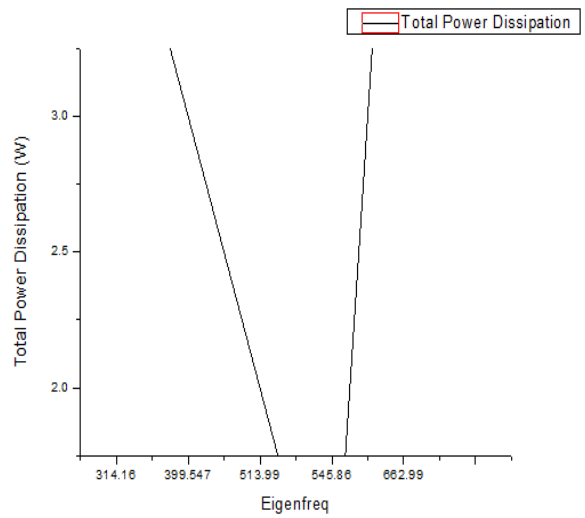
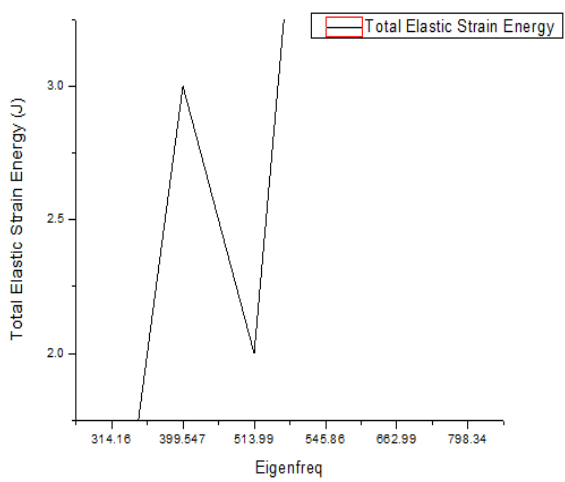


Fig 4.33 Total Elastic Strain Energy Vs Eigen Freq. Fig 4.33 Total P.D. Vs Eigen Freq.

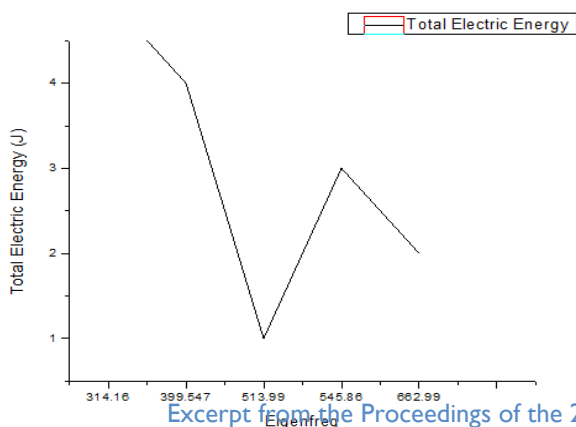


Fig 4.33 Total Electric Energy Vs Eigen Freq.

CONCLUSION:

Above project we have successfully completed initial learning of COMSOL and the design of aAIN BASED PRESSURE SENSOR using COMSOL.

REFERENCES:

[1] R. Weigel, *et al.*, "Microwave acoustic materials, devices and applications," *IEEE Transactions on microwave theory and techniques*, vol. 50, pp. 738-749, 2002.